



**HAL**  
open science

# New testing approach using near electromagnetic field probing intending to upgrade in-circuit testing of high density PCBAs

Nabil El-Belghiti, Patrick Tounsi, Alexandre Boyer, Arnaud Viard

## ► To cite this version:

Nabil El-Belghiti, Patrick Tounsi, Alexandre Boyer, Arnaud Viard. New testing approach using near electromagnetic field probing intending to upgrade in-circuit testing of high density PCBAs. 27th IEEE North Atlantic Test Workshop, May 2018, Essex, United States. 10.1109/NATW.2018.8388867 . hal-01997428

**HAL Id: hal-01997428**

**<https://hal.science/hal-01997428>**

Submitted on 29 Jan 2019

**HAL** is a multi-disciplinary open access archive for the deposit and dissemination of scientific research documents, whether they are published or not. The documents may come from teaching and research institutions in France or abroad, or from public or private research centers.

L'archive ouverte pluridisciplinaire **HAL**, est destinée au dépôt et à la diffusion de documents scientifiques de niveau recherche, publiés ou non, émanant des établissements d'enseignement et de recherche français ou étrangers, des laboratoires publics ou privés.

# New testing approach using near electromagnetic field probing intending to upgrade in-circuit testing of high density PCBAs

Nabil EL-BELGHITI ALAOUI  
Industrial Operations  
Department  
ACTIA Automotive  
CNRS, LAAS, 7 avenue du colonel  
Roche  
Toulouse, France  
[Nabil.elbelghiti-alaoui@actia.fr](mailto:Nabil.elbelghiti-alaoui@actia.fr)

Patrick TOUNSI  
CNRS, LAAS, 7 avenue du  
colonel Roche  
Univ. de Toulouse, INSA, LAAS,  
F-31400  
Toulouse, France  
[patrick.tounsi@laas.fr](mailto:patrick.tounsi@laas.fr)

Alexandre BOYER  
CNRS, LAAS, 7 avenue du  
colonel Roche  
Univ. de Toulouse, INSA, LAAS,  
F-31400  
Toulouse, France  
[aboyer@laas.fr](mailto:aboyer@laas.fr)

Arnaud VIARD  
Industrial Operations  
Department  
ACTIA Automotive  
Toulouse, France  
[arnaud.viard@actia.fr](mailto:arnaud.viard@actia.fr)

**Abstract**— With the density increase of today’s printed circuit board assemblies (PCBA), the electronic test methods reached their limits, in the same time the requirements of high reliability and robustness are greater. Original equipment manufacturers are obliged to reduce the number of physical test points and to find better-adapted test methods. Current test methods must be rethought to include a large panel of physical phenomena that can be used to detect electrical defects of components, absence, wrong value, and shorts at component level on the board under test (BUT). We will present the possibility of using electromagnetic signature to diagnose faulty components contactlessly. The technique consists in using small diameter near electromagnetic field probes, which detect the field distribution over powered sensitive components. A giant magnetoresistance (GMR) sensor was used as well to detect variations in low frequency components. The loading of the BUT is specifically chosen to enhance the sensitivity of the EM measurements. Reference EM signatures are extracted from a fault-free circuit, which will be compared to those extracted from a sample PCBA in which we introduced a component level defect by removing or changing the value of critical components. As a result, we will show that the amplitude of a specific harmonic acts as a sensing parameter, which is accurately related to the variation of the component value.

**Keywords**—Contactless testing, Near electromagnetic field, Design for testability, Accessibility, Testability, High density PCBA testing, statistical PCBA testing, Giant magnetoresistance sensors

## I. INTRODUCTION

During the assembly process of printed circuit boards, defects such as wrong value components, missing components, unwanted open circuits or short circuits may appear. Manufacturers continually look for faster, more accurate and more economical ways to identify this kind of defects. That’s why performing automated testing of dense populated printed circuit boards is a mandatory and cost effective solution to ensure manufacturing quality control.

Testing today’s populated PCBs is becoming increasingly challenging and more expensive as the use of small size surface mounted devices (SMD) is becoming predominant. The emergence of new technologies as High-Density Interconnect (HDI), embedded chips and Sequential Build-Up (SBU) circuit boards will even further increase the challenge for the test business.

Conventional techniques for automated PCBA testing involve applying signals through a number of test pins and measuring the output signals on the other test pins. Functional testing can be performed by energizing the PCBA, applying a predetermined number of input signals, and determining whether the proper output signals are generated by the circuitry on the BUT [1]. Alternatively, for a high volume manufacturing (HVM) process, a PCBA is tested primarily on a “bed-of-nails” fixture called in-circuit tester (ICT) that comprises pins called “nails” which directly contact the metallic traces on the BUT so that selected input signals may be applied at various test points (TP) on the PCB, and corresponding output signals can be measured on other TPs. This requires several physical TPs on the PCB traces which can compromise the integrity of the tested signals.

This widely used classical technique requires tight mechanical tolerances for the board layout, easily accessible test points and restricts the frequency band at which a board can be tested [2], which cannot be afforded anymore on a state of the art PCBA. Starting from this need, the idea of taking advantage of the HVM nature of the ICT and trying to upgrade it with contactless probes to meet current test challenges have come. In this paper, we present a new testing approach using EM near field sensors (NFS) to test populated PCBs.

After a presentation of the state of the art, the principle of the proposed method is given in order to understand its large scale application. To this aim and to prove the effectiveness of the method, we chose a DC/DC buck converter module as a case study. Simulations of value defect scenarios have been carried out on Cadence Orcad and validated by measurements

on the module in which we introduced controlled value defects on the input decoupling ceramic capacitors. First results to validate the principle and perspectives for future work are reported.

## II. STATE OF ART

Many research activities have been conducted to complement the actual ICT and eliminate its drawbacks while maximizing its effectiveness to follow the evolution of the PCBA industry. Probing techniques and inspection methods have been imagined by many researchers over the last 20 years. However, despite its immense ingenuity, they could not respond completely to the industrial constraints of testing high speed and high density PCBAs.

One printed circuit board probing technique for high speed and high density PCBAs is the bead probe technology, which is a micro access technique used to provide electrical access to PCBA for performing ICT. It uses small beads of solder placed onto the board traces to measure signals with a specific test probe. This access with standard ICT test pads is not feasible due to space constraints. A deficiency with this method is its capability to measure only signals located on the surface of the board which makes it unsuitable for testing high-density boards with many internal traces and buried vias [3]. Another deficiency is the soldering process which makes the mechanical contact less robust, thus the lifetime of the bead.

Other testing techniques based on providing electrical access for test to the traces located on the surface are the C.Vaucher method [4] and the test access component method by A.J.Suto [5]. Both techniques provide direct electrical contact to surface traces with either openings on the solder mask to create test points directly on PCB tracks using a conductive rubber tipped probe, or electrical surface mounted components. These two methods are limited by lifetime/cost and board space/complexity constraints.

An alternative inspection technique for high density PCBAs is the infrared thermal signature technique [6]. By classifying integrated circuits (IC) into a number of functional classes based on their thermal image, the PCBAs can also be classified into functional categories based on the classification of the ICs implemented on the board. It can detect and locate overstressed components and bridging faults. However, it requires long test time which can be unaffordable on an industrial product line.

Electromagnetic inspection techniques were subject to many researches and patents as well [7, 8]. One printed circuit board testing method is described in [9] disclosed stimulating a printed circuit board through the power and ground lines of the board with an AC signal and then contactlessly measuring the electromagnetic near field distribution proximate the board being tested. The electromagnetic “signature” of the board being tested was compared to the electromagnetic signature of a known good circuit board to determine whether the board under test was defective. Due to the complexity of printed circuit boards nowadays, this method can be less accurate and effective considering the size and density of current technology boards and digital circuits that needs precise levels of signal to be operational. The sensor plate used to measure the

electromagnetic signature is large and cannot be integrated into an In-circuit tester.

Thus there’s no method existing today that takes advantage of the classical ICT characteristics and upgrades its “probing by contact” structure to a contactless bed-of-nails structure.

## III. DESCRIPTION OF THE PROPOSED TESTING APPROACH

To improve the effectiveness and accessibility of current ICTs and gain accessibility to components that could not be tested without placing numerous test points, we propose in this article a new test approach based on EM inspection using near field sensors as an upgrade to the classical In-circuit testers. With near field measurements above PCBA components, contactless information about charge and current distribution can be obtained without access limitation on the PCBA surface.

### A. Principle

The principle of this method (see Fig.1) is to measure the EM near field distribution directly over the center of a powered component contactlessly and compare the measured electromagnetic signature (EMS) to a database of correct signatures pre-established on a fault-free PCBA. The measured electric and magnetic fields (EMF) are generated by the distribution of charges and currents respectively in the components of the BUT. Accurate and repeatable measurements of these fields produce a specific time and frequency domain signature for each critical component, which can be extended to a complete operational block, and then to the complete board in a further application. Such signatures are then compared to a pre-established non-faulty signature pattern of the same type of board to determine whether the BUT is faulty or not and pinpoint exactly where the faulty component is located knowing the position of the NFS on the board.

Thus firstly, the board or the operational block of the board is powered and operates normally. The electromagnetic near-field distribution generated by every “critical” component on the block is then detected using non-contact NFS mounted directly over these components in a bed-of-nails structure. The registered signature specific to the component and the conditions of the excitation of the electronic block is registered and subsequently compared with a sample signature of the same block in a non-faulty board, which was registered in the same excitation conditions to determine whether the response is in conformance with the known reference.

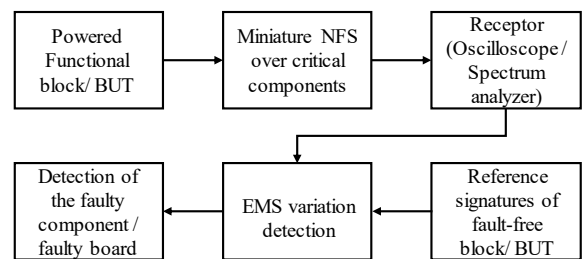


Fig. 1. Principle of the near field probing test approach

### B. Types of detected assembly defects

The defects that can be detected with this method are at component level. In other words, starting from the hypothesis that the bare PCB is fault free guaranteed from the printed circuit manufacturer, or had already been tested and certified non-faulty. We can detect assembly defects over critical components: presence, polarity for components that exhibits field change when mounted in reverse polarizations, value, a wrong package that can change the height of the component, overstressed/overheating components and solder defect (open and shorts). These components must be carefully chosen in advance in order to establish design for testability rules (DFT) to minimize the probe count and maximize fault detection on a functional block level.

## IV. CASE STUDY: DC/DC BUCK CONVERTER

To validate our approach, we chose a DC/DC converter because of the important transient currents crossing the critical components when the module is powered. Components such as input/output filtering capacitors, MOSFETS and inductors radiate a significant high frequency magnetic field in the near field region due to the large transient currents crossing them. The currents and the induced magnetic fields are related to component values, package and mounting. From the analysis of measured magnetic fields, the presence and the location of assembly defects or wrong components can be detected.

This case represents a scenario of testing a DC/DC module in a power management block of an industrial high density PCBA using the EMF radiated from its critical components. Using a commercial near field probe (NFP), the EM signature of critical components that have a high frequency transient current passing through them, as described above, is registered to establish a sample signature of each component.

We chose an off-the shelf (OTS) evaluation board of a synchronous DC/DC buck converter module with a fully integrated controller to run tests. The powering conditions for test are as mentioned in Table I.

TABLE I. POWERING CONDITIONS FOR TEST

$V_{in}$	20 V
$V_{out}$	12 V
$I_{Load}$	3 A
Frequency	250 kHz

### A. Simulated defect scenarios:

The first defect scenario used to validate this approach is the detection of a wrong value of an input decoupling capacitor. The approach is tested initially in simulation, and then validated in measurement.

#### 1) Test procedure: Simulation

We modeled the DC/DC evaluation board on *Cadence-Orcad* using the *pspice* model of the controller given by the manufacturer (see Fig.2). Estimated values of parasitic elements of each critical component were used to give a more accurate and “realistic” simulation result. Then, we ran multiple parametric simulations of the value of each input

capacitor with four different values (see Table II) to evaluate how the derivative of the current in each input capacitor reacting to a change of value of an input capacitor and the induced variation over the other capacitors that have correct values. The derivative of the current in a component represents the image of the magnetic field measured with a commercial NFP over this specific component.

TABLE II. VALUES USED FOR INPUT CAPACITORS IN SIMULATION AND EXPERIMENTS

Input capacitors	Correct value ( $\mu F$ )	Incorrect values ( $\mu F$ )
C8	2.2 $\mu F$	1, 1.5, 3.3, 15
C9	2.2 $\mu F$	1, 1.5, 3.3, 15
C10	2.2 $\mu F$	1, 1.5, 3.3, 15
C11	2.2 $\mu F$	1, 1.5, 3.3, 15
C22	47 $\mu F$	unchanged

#### 2) Test procedure: Experimentation

We reproduced the same scenario described in the test procedure simulation with the same values on the evaluation DC/DC module. We changed the value of each input capacitor on the board several times by soldering and removing a different value capacitor for every input ceramic capacitor (C8,C9,C10,C11), and we collected the time domain signatures over each capacitor using an oscilloscope for each of the four values evaluated. Collected signatures of each capacitor were analyzed to evaluate their variance compared to the reference signatures.

#### 3) Test bench description

##### - Near field probes

Measuring the time domain H-field signatures over the powered (see Table I) DC/DC buck-converter was carried out using a commercial mini (resolution <1mm) Near-Field probe (LANGER RF-R 0.3-3) (see Fig.4) which measures magnetic fields in the range of 30MHz to 3GHz. The probe was directly connected to a digital oscilloscope with 50 $\Omega$  impedance. The NFP was then freely and accurately moved over every input capacitor at a 2mm distance of the center of the component using an automatic computer controlled scan table with a distance precision of 25 $\mu m$  (see Fig. 3).

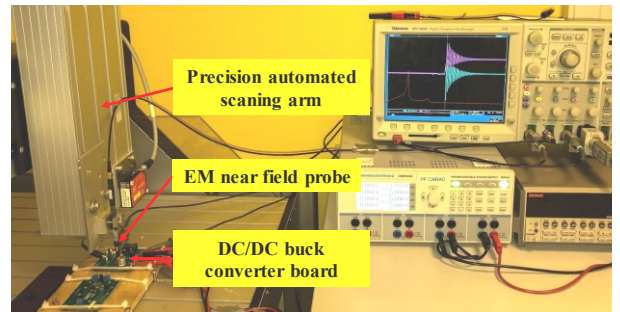


Fig. 3. Test bench set-up

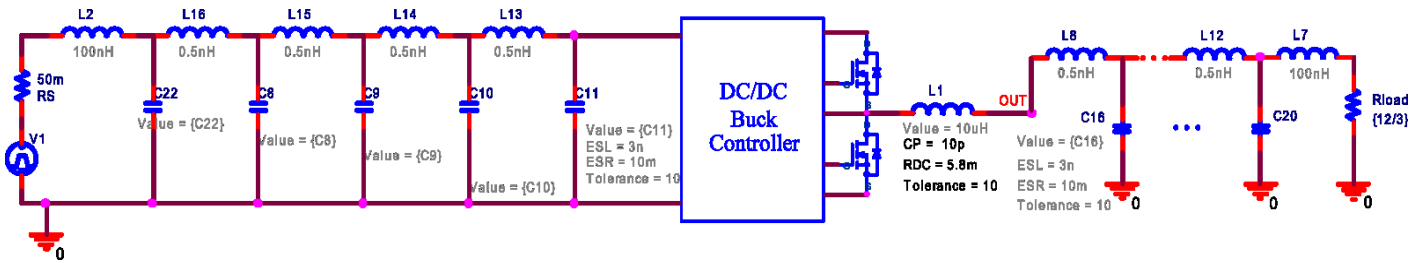


Fig. 2. Simplified schematic of simulation

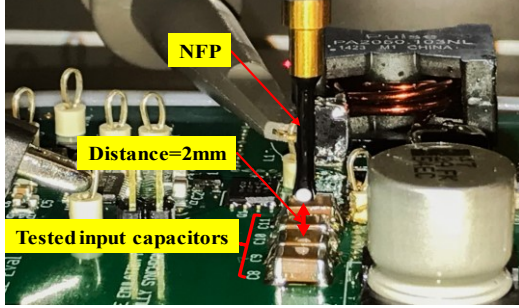


Fig. 4. Close-up showing the NFP and the probed components

Near field probes have a high sensitivity when measuring high frequency fields, on the other hand, low frequency fields are not detected. To compensate the lack of sensitivity in low frequency measurements, another type of NFS is introduced in the following paragraph.

- *GMR Sensors*

The giant magnetoresistance effect (GMR effect) discovered in 1988 [10] is related to field dependent changes in resistance that can be observed in thin-film ferromagnetic/non-magnetic metallic multilayers. The term GMR was coined since the large change in resistance (10 to 20%) in the thin-film materials. In the field of magnetic sensing, GMR sensors have taken an important role due to their small size, high signal level, high sensitivity, large frequency response and low cost [11].

In our attempt to improve ICT using a contactless near field measurement method, in addition to the NFP previously used to detect value changes in components in which we have high frequency transient currents passing through, we tested the use of a GMR sensor. This sensor technology provides an important sensitivity for relatively low frequency magnetic fields (up to 1MHz) [12], which is the case of the inductor in a DC/DC buck converter. The low frequency current ripple in the inductor can be measured with a GMR sensor to detect the value variation of the inductor under test.

- *Sensor used :*

The GMR sensor used is a commercial multilayer GMR sensor that has a sensitivity of 5.4 mV/V/A for frequencies up to 100 KHz. A dynamic characterization of the sensor shows a sensitivity drop of 3.16 mV/V/A per decade for greater frequencies.

At around 400 KHz, the switching frequency of this converter, the sensitivity of the sensor ( $S_{dynamic}$ ) is estimated at 3.8 mV/V/A. The sensor was biased with a 20V power supply. Knowing that the level of the fields measured will not push the signal out of the linear range; we used a small magnet to polarize the sensor in its linear region (see Fig. 5).

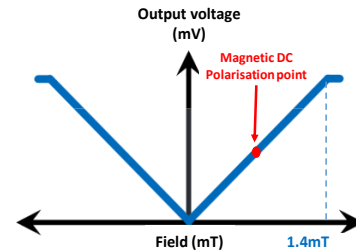


Fig. 5. Idealized transfer function of the GMR sensor used

In this particular sensor, four GMR resistors are configured as a Wheatstone bridge [13], which provides a voltage output that is proportional to the magnetic field measured. Two of the resistors are sensing resistors (R2 and R4) (see Fig. 6); the other two are reference resistors. In response to an external magnetic field, the resistance of the exposed sensing resistors decreases while the reference resistors remain unchanged, causing a voltage at the bridge output.

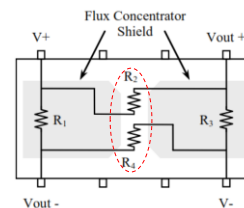


Fig. 6. Commercial GMR sensor configuration

- *Test conditions :*

We used the commercial GMR sensor to test a 2525 SMD inductor mounted on a different DC/DC Buck converter evaluation module (see Table III).

The measurements were taken at a distance of  $d=2\text{mm}$  from the surface of the inductor for four different values (see Fig. 7). The converter was powered on, and the output load current was constant at 3A. The GMR sensor was polarized using a small rectangular magnet. Table III summarizes test conditions.

TABLE III. TEST CONDITIONS

$V_{in\_DC/DC}$	10V
$V_{out\_DC/DC}$	1.2V
$V_{supply\_GMR}$	20V
$F_{sw}$	400KHz
$I_{Load}$	3A
Inductor reference value	$L=0,47\mu H$
Inductor wrong values to be detected	$L=0,22\mu H$
	$L= 82\mu H$
	$L= 1,5\mu H$

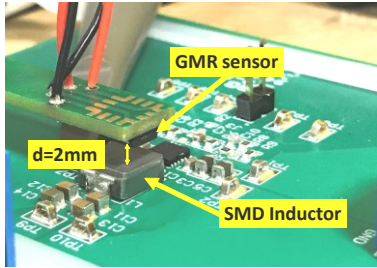


Fig. 7. Image of the GMR sensor and the measured SMD inductor

## V. SIMULATION AND EXPERIMENTAL RESULTS

### A. Above the input decoupling capacitors

#### 1) Reference signatures:

The reference signature is the EMF measured over each input capacitor when it has a correct value. Figure 8 shows a great coherence between the simulation results and the measurement results over input capacitors C8, C9, C10, and C11. The difference in the frequency scale is due to assumptions made on the parasitic parameters of the components in the simulation model to be considered in the future work.

The difference of amplitudes between simulation (dashed lines) and measurement (solid lines) is due to the coupling parameter of the NFP that wasn't taken into account in the simulation model.

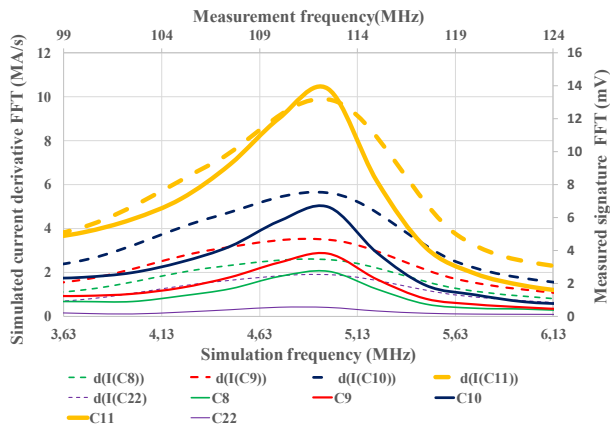


Fig. 8. Simulated current derivatives FFT of input capacitors (dashed lines), (vs) measured EM signatures FFT on the buck converter PCB

#### 2) Signatures with wrong values of the input capacitors

In concerns of conciseness, only the signatures measured over all input capacitors induced from the variation of the value of the input capacitor C8 will be presented in this section (see Fig. 9 and Fig. 10).

The dashed lines show the small signature variations of the unchanged input capacitors (C9, C10, C11, C22). Bold lines are the variation of C8 signatures when we varied its value. Results from simulation and measurements show that C8 EM signature varies significantly, while the other capacitors signature stays roughly unchanged.

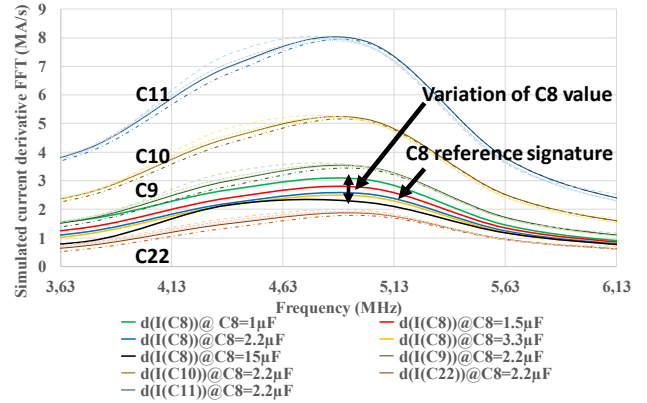


Fig. 9. Simulated current derivatives FFT of input capacitors when C8 varies

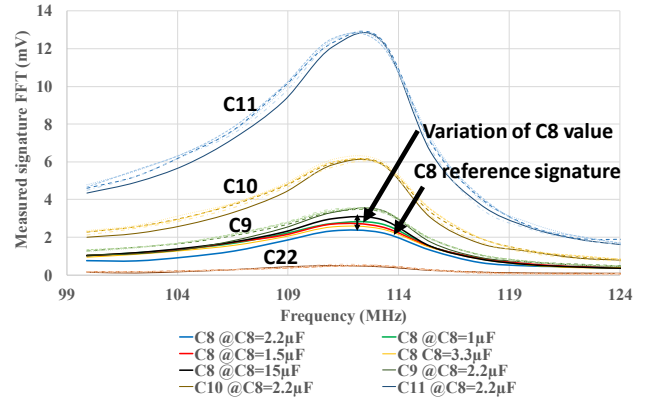


Fig. 10. Measured EM signatures FFT of the input capacitors when C8 varies

#### 3) Comparison and analysis

From the measurement results we can see that the capacitor value change induces a significant variation on the amplitude spectrum at around 110MHz of the EM signature of the capacitor being changed. This frequency represents the resonance of the input capacitors with the parasitic elements of the switching stage of the converter. It varies according to the board under test.

This is still true for all input capacitors when we change their value. They all exhibit a significant variance of their spectrum amplitude signature at around 110MHz.

These results can be summarized in the graph below (see Fig. 11), which shows that the most scattered signatures around the reference are those of the decoupling capacitor for

which the value was changed. The dispersion of signatures remains lower for all fixed capacitors.

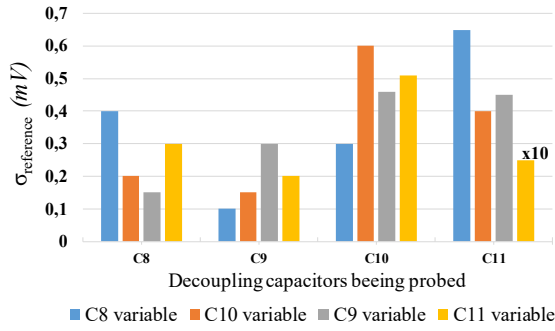


Fig. 11. Standard deviation of the measured amplitude spectrum EM signature in each case where the value of one input capacitor is changed separately

<sup>x10</sup> The value of this deviation is 2mV, it was divided by 10 to fit in the comparison graph.

### B. Above the output filter capacitors

The output capacitance of a switching DC/DC converter is a vital part of the overall feedback system. The energy storage inductor and the output capacitors form a second-order low-pass filter. The output filter's inductor therefore limits the current slew rate. When the amount of current required by the load changes, the initial current deficit must be supplied by the output capacitors until the regulator can meet the load demand [14].

To measure NF signatures over these output capacitors forming the LP filter we need to emphasize on their effect by pushing them to provide a high transient current to the load.

To do so, we designed a PCB that provides a current step by switching the output current of the converter between two different load resistors R17 and R18 (see Fig. 12). The load current switches between 50mA and 2.5A with a rising time of 1 μs and a falling time of 0.5 μs.

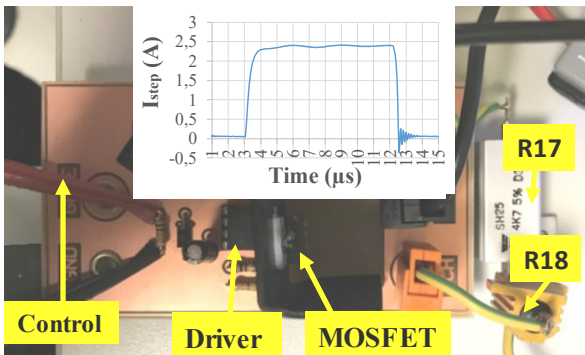


Fig. 12. Load transient current PCB

#### 1) Signatures with wrong values of the output capacitors

Near field signature measurements over each changing output capacitor (see Table IV) show clearly which capacitor's value is being changed. Only the signatures measured over the

accessible top board capacitors (C16 and C20) are here presented (see Fig. 13 and Fig. 14).

The dashed lines show the small signature variations of the unchanged output capacitors. Bold lines are signature variations of the changed output capacitor.

TABLE IV. VALUES USED FOR THE OUTPUT CAPACITORS

Input capacitors	Correct value (μF)	Incorrect values (μF)
C16	47 μF	22, 33, 68
C20	22 μF	10, 15, 33

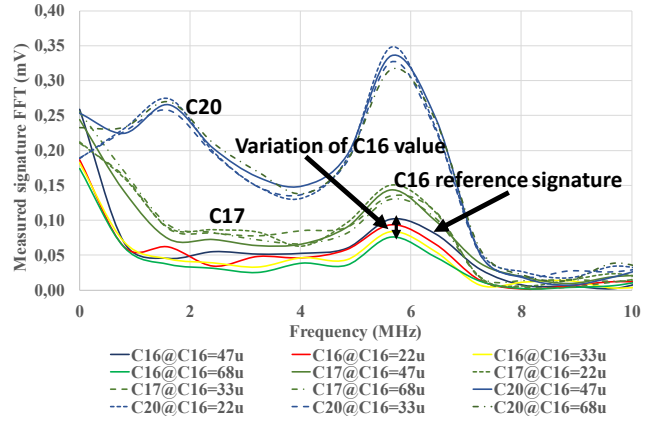


Fig. 13. Measured EM signatures FFT of the output capacitors when C16 varies

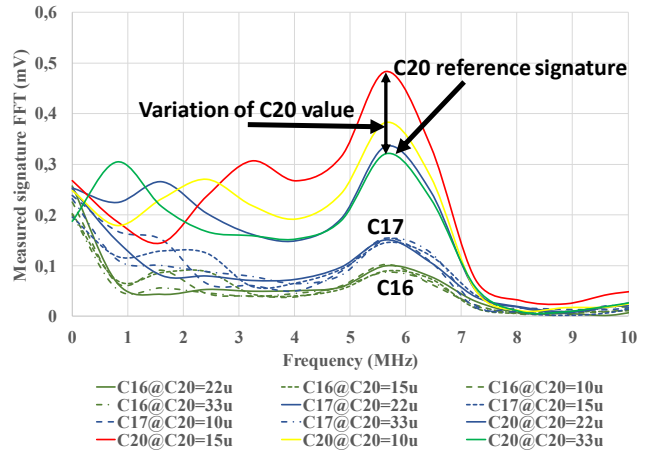


Fig. 14. Measured EM signatures FFT of the output capacitors when C20 varies

We can clearly distinguish the capacitor that have a wrong value from the amplitude of its signature deviating from the reference one. This measured signature is the resonance of the loop composed of the output capacitors and the current step PCB parasitic elements (track inductances and switch parasitic capacitances). In this particular case, we observed the resonance at 5.5MHz. This frequency depends on the output capacitors under test and the parasitic elements of the circuit creating the test stimulus (current step PCB in this case).

### C. Above the output filter inductance using a GMR sensor

The results presented below (see Fig. 15) show the possibility to detect variations of the value of the inductor using a GMR sensor. The peak-to-peak amplitude of the sensor's output voltage doubles as the value of the inductor is divided by 2, which is coherent since the sensors output has a linear relationship with the AC magnetic field ( $B$ ) created by the current ripple ( $\Delta I_L$ ) in the inductor (see equation (1)).

$$V_{out_{GMR}} = S_{dynamic}(f) \times B \propto (\Delta I_L) \quad (1)$$

$$\Delta I_L = \frac{1}{F_{sw} \times L} V_{out_{DC/DC}} \left( 1 - \frac{V_{out_{DC/DC}}}{V_{in}} \right) \quad (2)$$

$F_{sw}$  is the converter's switching frequency and  $L$  is the value of the filtering inductance. All measurements are in raw conditions, no shielding, filtering or amplification were used.

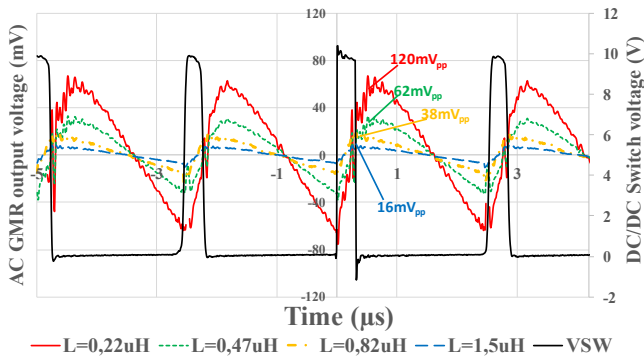


Fig. 15. Output voltage of the GMR sensor showing the variation of the inductor's value

The sensor's AC output voltages reflects the waveform of the current ripple in the inductor, which is inversely related to the value of the inductance (see equation (2)). Table V resumes the results presented in Fig. 15.

The measurement of the magnetic field above the inductor, and the comparison with the measurement on a reference sample makes it possible to detect a bad mounted value without the need for test points.

TABLE V. SENSOR OUTPUT VOLTAGE ACCORDING TO INDUCTOR'S VALUES

Value of the inductance ( $\mu\text{H}$ )	Sensors output voltage ( $\text{mV}_{pp}$ )
0,22	120
0,47 (reference value)	62
0,82	38
1,5	16

### VI. CONCLUSION AND FUTURE WORK:

We presented the possibility of using electromagnetic signature to diagnose faulty components contactlessly on a limited physical access PCBA.

To validate the principle we used miniature near electromagnetic field probes to measure magnetic field

distributions over powered sensitive components and to give insight on the value of the component and its solder condition (soldered or non-soldered). The loading of the BUT was specifically chosen to enhance the sensitivity of the EM measurements. For the decoupling capacitors a normal powering of the BUT was used. For the output filtering capacitors a high transient load current was used as a stimulus to enhance the effect of these capacitors on the NF measured.

These raw measurement results showed that the amplitude of the first resonance harmonic on the spectral signature acts as a sensing parameter, accurately related to the variation of the component value.

Measuring the variation of the inductance value was evaluated using a commercial GMR sensor which was previously characterized to obtain its dynamic sensitivity. We showed the possibility to distinguish the variation of the inductance value based on the voltage drop/increase observed in the sensors output voltage.

This first experimental results demonstrate that the near field probing approach here presented can provide a viable option to detecting specific component level defects and decreasing the number of traditional test points while still providing access. Experiments are still on-going to validate the approach on large scale applications. A proper amplification and signal conditioning will be considered in a future work to increase measurement sensitivity and to set detection limits.

### REFERENCES

- [1] Robinson/Verma, "Optimizing Test Strategies during PCB Design For Boards with Limited ICT Access", Proceedings of the Telecom Hardware Solutions Conference, May 2002
- [2] D.Gizopoulos, Advances in Electronic Testing: Challenges and Methodologies. New York: Springer, 2006. P.371
- [3] J. McMahon, T. Blaszczyk, P. Barber, "Implementing Robust Bead Probe Test Processes into Standard Pb-Free Assembly," IPC APEX EXPO Conference, Proceedings, 2013
- [4] C.Vaucher and L. Balme, "Analog/digital testing of loaded boards without dedicated test points," in Proceedings International Test Conference 1996. Test and Design Validity, 1996, pp. 325–332.
- [5] Test access component for automatic testing of circuit assemblies, A.J.Suto, US patent application 20100207651
- [6] H. Moldovan, M. Marcu, and M. Vladutiu, "PCB Testing Using Infrared Thermal Signatures," in 2005 IEEE Instrumentation and Measurement Technology Conference Proceedings, 2005, vol. 3, pp. 1970–1974.
- [7] Method for testing printed and unprinted circuit board assemblies aligning a focused, high-frequency electromagnetic transmission beam to irradiate a component to be tested and produce a spectral measuring signal, R.Wein, DE19837169A1
- [8] Method and apparatus for high-speed scanning of electromagnetic emission levels, G.Gunthorpe & D.James, WO1997017617A1
- [9] Contactless test method and system for testing printed circuit boards, J.Soiferman, US5517110A
- [10] M.N Baibich, J.M. Broto, A. Fert, F. Nguyen Van Dau, F. Petroff et al « giant magnetoresistance of (001)Fe/(001)Cr magnetic superlattice,» *Phys. Rev. Lett.* vol.61, no. 21, pp. 2472-2475, 1988
- [11] A. Bernieri, G. Betta, L. Ferrigno, M. Laracca, "Improving performance of GMR sensors", *IEEE Sensors J.*, vol. 13, no. 11, pp. 4513-4521, Nov. 2013.
- [12] D. Cubells-Beltran, M & Reig, Candid & Martos, J & Torres, Jose & J. Soret, "Limitations of Magnetoresistive Current Sensors in Industrial

Electronics Applications". INTERNATIONAL REVIEW OF ELECTRICAL ENGINEERING-IREE. 6. 423-429, 2011

- [13] P. Ripka, M. Janosek, "Advances in magnetic field sensors", *IEEE Sensors J.*, vol. 10, no. 6, pp. 1108-1116, Jun. 2010
- [14] <http://www.ti.com/lit/an/slta055/slta055.pdf>